MRS Advances (2023) 8:693–697
https://doi.org/10.1557/s43580-023-00581-7

ORIGINAL PAPER

Influence of MnTe inclusions on thermoelectric properties of Fe_2TiSn

Kseniia Scherbakova[1] · Aleksandra Khanina[1] · Andrei Novitskii[1,2] · Illia Serhiienko[2,3] · Aleksandr Shubin[1] · Oleg Ivanov[1,4] · Nikolay Repnikov[4] · Vladimir Khovaylo[1]

Received: 24 February 2023 / Accepted: 3 May 2023 / Published online: 9 May 2023

Abstract
Thermoelectric properties of composites consisting of antiferromagnetic MnTe as inclusion and Fe_2TiSn Heusler alloy as a thermoelectric matrix were studied. Samples of $Fe_2TiSn + x$MnTe ($x = 0$, 2, 4, and 6 wt.%) were obtained by mixing Fe_2TiSn and MnTe powders in planetary mill and subsequent consolidation by Spark Plasma Sintering. Measurements of thermoelectric properties revealed a decrease of thermal conductivity with an increase in the mass fraction of MnTe in the studied composites, which was ascribed to the enhanced phonon scattering at the matrix/inclusion interfaces. However, due to the decrease in the electrical conductivity and the Seebeck coefficient, the thermoelectric figure of merit ZT is significantly reduced in the studied composites.

Introduction

Recently, the development of alternative environmentally friendly energy conversion technologies has attracted growing interest. Among the various energy conversion technologies, special attention has been paid to devices based on thermoelectric (TE) materials that can directly convert thermal energy in electrical one. TE materials can be used for heat recovery in many industrial or civil facilities, such as cars, thermal power plants, blast furnaces, etc. [1]. Efficiency of this conversion is directly related to the so-called figure of merit zT of a thermoelectric material, which is determined as

$$zT = \frac{S^2\sigma}{\kappa}T,$$

where σ is electrical conductivity, S is Seebeck coefficient, κ is thermal conductivity and T is the absolute temperature.

✉ Vladimir Khovaylo
khovaylo@misis.ru

1 National University of Science and Technology "MISIS", Moscow 119049, Russia

2 International Center for Materials Nanoarchitectonics (WPI-MANA), National Institute for Materials Science, Tsukuba, Ibaraki 305-0044, Japan

3 Graduate School of Pure and Applied Sciences, University of Tsukuba, Tsukuba, Ibaraki 305-8573, Japan

4 Belgorod State University, Belgorod 308015, Russia

Among a large family of TE materials studied in 1960s and 1970s, binary compounds based on lead telluride and bismuth telluride had attracted special attention. Although these compounds have still been considered as good materials for thermoelectric applications due to their high figure of merit, the toxicity of lead has prompted scientists and engineers to look for more environmentally friendly compounds for thermoelectric devices. Among the stable binary compounds of manganese, only MnTe exhibits semiconductor properties [2].

MnTe has been intensively studied since 1960s, but the complexity of samples preparation and its antiferromagnetic nature, which persists even above room temperature, prevented its use as thermoelectric materials. Now, antiferromagnetic properties of MnTe have been actively studied in view of their possible use in spintronic devices. In addition, the combination of thin-film α-MnTe with a topological insulator, which constitutes antiferromagnetic spintronic systems, demonstrates a unique behavior and provides advantages such as energy independence, terahertz spin dynamics, absence of edge stray fields and resistance to magnetic fields, thus being capable of operating beyond the Moore's law [3].

The crystal structure of compounds based on manganese telluride belongs to the B81 NiAs (α-MnTe) structure type [4]. MnTe is a p-type semiconductor with a direct band gap of 1.27 eV [2], an indirect band gap of 0.8 eV in antiferromagnetic [5] and 0.4 eV in the paramagnetic state [6]. Relatively low lattice thermal conductivity of 0.66 $W \cdot m^{-1}\ K^{-1}$ at high temperatures [7] makes it possible to consider MnTe

as a potential fuel cell material. However, the high Seebeck coefficient of MnTe is usually accompanied by a low charge carriers concentration of ~ 10^{18} cm^{-3}, which degrades electrical conductivity and other electrical transport characteristics. Therefore, much of the effort has gone into developing new methods and strategies to improve the thermoelectric power factor $PF = S^2\sigma$ of MnTe.

Research on thermoelectric properties of MnTe dates back to the 1960s when Na was used to control hole concentration and its peak value of zT was estimated to be 0.4 [8]. To date, many simple strategies are already known to increase zT by increasing the power factor and reducing the thermal conductivity of the lattice. One major strategy has been developed to effectively improve power factor through band engineering [9–11], typified by resonant doping [12], filtering effect [13, 14], and modulation doping [15]. Another strategy can be implemented using several approaches, including defect engineering [3] and nanostructures [13] for phonon scattering, which leads to a significant decrease in the lattice component of thermal conductivity and, thus, to an increase in zT.

Kim et al. [15] reported a decrease in thermal conductivity in non-stoichiometric manganese telluride compounds with increasing Mn content and demonstrated a zT value of 0.41 at 773 K for a non-stoichiometric $Mn_{0.51}Te_{0.49}$ obtained by spark plasma sintering. Later, by increasing the concentration of charge carriers, zT equal to 0.59 was obtained by Zhang et al. [16] for a sample with a reduced content of manganese $Mn_{0.98}Te$. It was demonstrated recently [17] that the doping of manganese telluride with Sn leads to an increase in the concentration of charge carriers, which improves the electrical properties, and introduces additional phonon scattering on point defects and mass fluctuations, leading to a decrease in thermal conductivity. Thus, the thermoelectric characteristics were improved, and the maximum zT of about 0.93 at 873 K was achieved for a $Mn_{1.02}Sn_{0.04}Te$ sample [17]. Subsequently, the zT value was increased to 1.2 at 873 K in a MnTe + 1.5 at.% Sb_2Te_3 sample by introducing Sb_2Te_3 into manganese telluride matrix [18]. Doping with sodium results in zT greater than unity at 873 K [19]. The introduction of a Ag_2S phase into manganese telluride leads to a significant decrease in thermal conductivity (about 50%), while a partial replacement of Mn by Ag and Te by S leads to an improvement in the electrical conductivity due to an increase in the concentration of charge carriers. The combination of these two effects made it possible to increase the value of zT to 1.1 [20].

Speaking about MnTe-based composite thermoelectrics, so far activities in this direction have been restricted to the case of in situ formed nanoprecipitates of MnTe in the matrix of host material. Tan et al. [21] reported that the relatively high solubility of MnTe in SnTe allows for heavy doping to form MnTe nanoprecipitates, which can significantly improve the electrical and thermal transport properties of SnTe through band structure engineering, multiple phonon scattering, and suppression of bipolar thermal conduction [21]. Based on the same strategy, the thermoelectric properties of PbTe were improved, where a large amount of MnTe nanoprecipitates causes an energy filtering effect to improve the Seebeck coefficient. Also, it has been shown [22] that doping with MnTe increases the scattering in GeTe, which leads to a very low thermal conductivity of the lattice of the order of 0.250.5 Wm^{-1} K^{-1}, and the combination with antimony also increases the mechanical strength of the alloy [23]. As a result, the largest value of zT was 1.61 at 823 K for the $Ge_{0.86}Mn_{0.10}Sb_{0.04}Te$ compound.

In our work we studied influence of MnTe on thermoelectric properties of Fe_2TiSn full-Heusler alloys. Specifically, we prepared a series of $Fe_2TiSn + x$MnTe samples, where $x = 0$, 2, 4, and 6 wt.% and investigated thermoelectric properties of these composites.

Materials and methods

Polycrystalline ingot of Fe_2TiSn was prepared by arc melting method using pure (at least 99.99%) constituting chemical elements. Rapidly quenched ribbons of Fe_2TiSn were produced by melt-spinning method (Melt Spinner MSP 10, Edmund Buehler GmbH). The obtained ribbons were then crushed into fine powder by ball milling (Fritsch Pulverisette 7 premium line). An ingot of MnTe was prepared by solid state synthesis in evacuated quartz ampule. The ingot was ground into fine powder by the ball milling. Experimental samples of thermoelectric composites $Fe_2TiSn + x$MnTe ($x = 0$, 2, 4, and 6 wt.%) were obtained by mixing Fe_2TiSn and MnTe powders in planetary ball miller and subsequent consolidation of the samples by Spark Plasma Sintering (SPS, Labox 650 Sinter Land).

Crystal structure of the samples was investigated at room temperature on powdered samples by the X-ray diffraction (XRD) analysis using Cr-Kα source (λ = 0.2291 nm). Thermal conductivity was calculated from the experimental results of thermal diffusivity, measured by laser flash method (LFA 467, Netzsch), specific heat and density of the samples. Seebeck coefficient and electrical conductivity were measured simultaneously by differential and four-probe methods, respectively, by using a home-made equipment.

Results and discussion

X-ray diffraction pattern taken from the composite samples $Fe_2TiSn + x$MnTe ($x = 0$, 2, 4, and 6 wt.%) at room temperature is shown in Fig. 1. Calculated from the XRD data lattice parameter of the Fe_2TiSn matrix was found to be

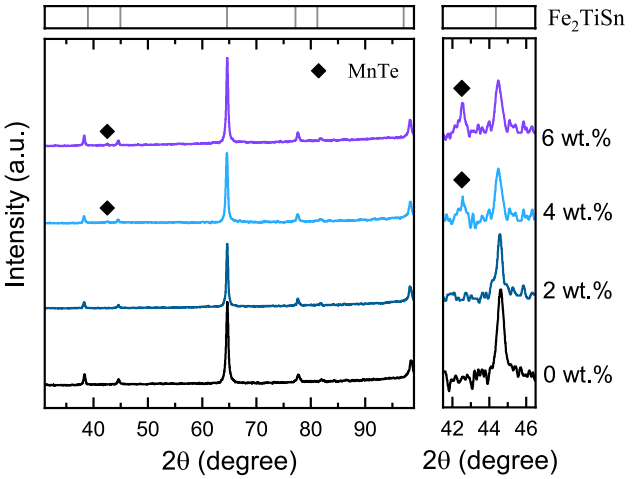

Fig. 1 X-ray diffraction patterns of $Fe_2TiSn + x$MnTe ($x = 0$, 2, 4, and 6 wt.%) composites. Peaks position from the cubic Heusler structure is shown on the top

$a = 0.6057$ nm. This value is in a good agreement with that reported in the literature [24]. It is seen that in the case of samples containing 0 and 2 wt.% of MnTe, only the peaks characteristic of the Fe_2TiSn Heusler phase are observed. A peak from MnTe becomes visible on the XRD pattern of the $x = 4$ wt.% sample (see enlarged view on right panel of Fig. 1). It should be noted that no shift of the peaks position of the Fe_2TiSn matrix is observed, which means that when inclusions of manganese telluride are added, there is no incorporation or replacement of atoms in the cubic structure of Fe_2TiSn. It can be concluded therefore, that there is no reaction between the Fe_2TiSn matrix and the MnTe filler.

The temperature dependences of the electrical conductivity σ, Seebeck coefficient S, and power factor $PF = S^2\sigma$ of the synthesized composite samples are shown in Fig. 2. For the Fe_2TiSn Heusler alloy sample without inclusions, the obtained data are comparable with the literature data [25–28]. The electrical conductivity tends to decrease to 300 K, which is inherent for metals, then, with increasing temperature, it begins to increase and becomes characteristic of semiconductor compounds. The Seebeck coefficient has a bell-shaped dependence with a maximum of about 29 $\mu V \cdot K^{-1}$ at 300 K. The power factor behaves similarly, having a peak of 2.31 $\mu Wcm^{-1} K^{-2}$ at the same temperature.

An increase in the amount of filler leads to a decrease in all the thermoelectric characteristics. The decrease in electrical conductivity values can be described by the disorder of the resulting structure, which prevents conduction. It can be seen that samples with 4 and 6 wt.% of MnTe have the same electrical conductivity. The Seebeck coefficient S and power factor PF also decrease significantly. The peaks of S shifts towards lower temperatures, down to ~ 200 K in the samples with MnTe addition.

The temperatures dependences of the total κ, electronic κ_{el}, and lattice κ_{lat} thermal conductivities of the synthesized composite samples are shown in Fig. 3. The total thermal conductivity decreases with an increase in the fraction of MnTe inclusions, which may indicate an increase in phonon scattering at the matrix/inclusion interfaces. As the temperature increases, the total thermal conductivity κ increase linearly, this tendency arises due to the fact that the electronic component begins to make a more significant contribution to the overall thermal conductivity than the lattice component. In general, the total, electronic and lattice thermal conductivity decrease with increase in MnTe volume fraction, which is related to enhanced phonon scatterings at the grain boundaries and interfaces between the Fe_2TiSn matrix and MnTe inclusions.

The temperature dependence of the thermoelectric figure of merit zT of the synthesized composite samples is shown in Fig. 4. It is seen that addition of MnTe to the host Fe_2TiSn strongly decrease the figure of merit. It is due to the fact, that both electrical conductivity and Seebeck coefficient, which largely determine zT, are strongly suppressed by MnTe addition.

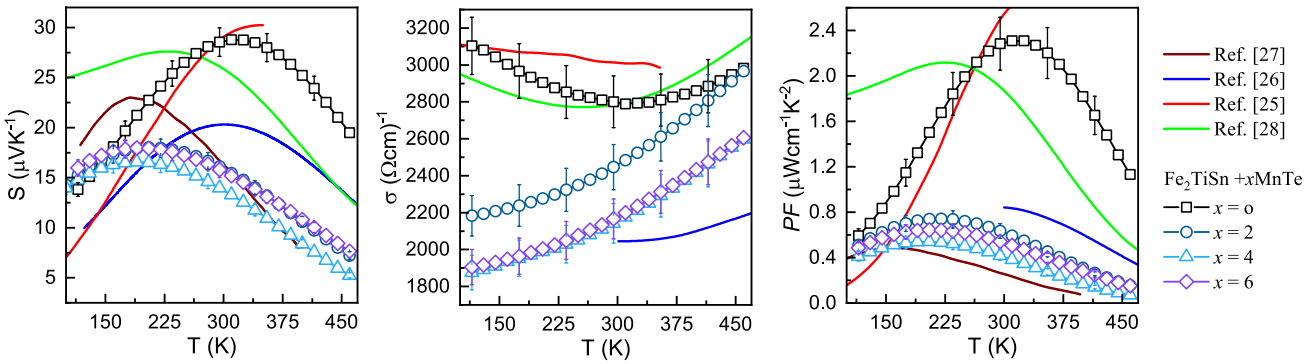

Fig. 2 Temperature dependences of Seebeck coefficient (left panel), electrical conductivity (central panel), and power factor (right panel) for $Fe_2TiSn + x$MnTe ($x = 0$, 2, 4, and 6 wt.%)

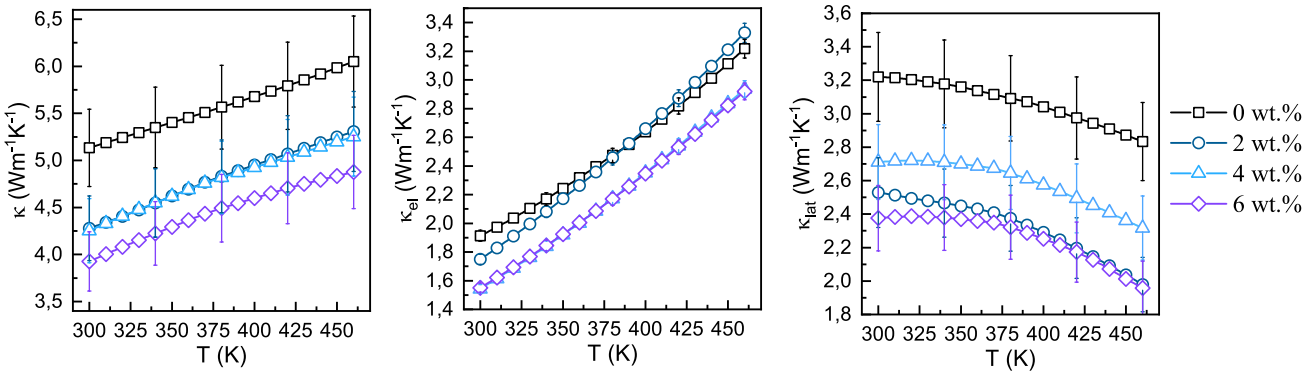

Fig. 3 Temperature dependences of total κ (left panel), electronic κ_{el} (central panel), and lattice κ_{lat} (right panel) thermal conductivities in $Fe_2TiSn+x$MnTe ($x=0$, 2, 4, and 6 wt.%)

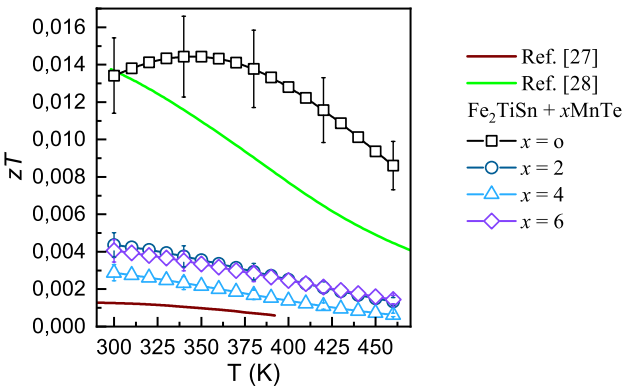

Fig. 4 Temperature dependence of thermoelectric figure of merit zT. For comparison, data from the literature sources are given [27, 28]

Conclusion

In conclusion, we prepared thermoelectric composite based on Fe_2TiSn Heusler alloy as a matrix and MnTe powder as a filler. Investigation of thermoelectric properties of the prepared composites showed that with an increase in the mass fraction of MnTe, the absolute values of electrical conductivity σ and Seebeck coefficient S decrease. The decrease of σ in the studied composites is mainly due to enhanced charge carriers scattering, which is common to composite materials, as well as to the rather poor electrical conductivity of MnTe at temperatures below 500 K [15]. The thermal conductivity of the studied composites decreases as well, which is presumably due to the enhanced phonon scattering at the matrix/inclusion interfaces. Due to the detrimental impact of the decrease in S and σ, the thermoelectric figure of merit ZT in the studied $Fe_2TiSn+x$MnTe composites significantly decrease.

Funding This work was supported by the Russian Science Foundation (Grant No. 21-12-00405).

Declarations

Conflict of interest The authors declare that they have no conflict of interest.

References

1. L.E. Bell, Science **321**, 1457 (2008)
2. W. Szuszkiewicz, E. Dynowska, B. Witkowska, B. Hennion, Phys. Rev. B **73**, 104403 (2006)
3. S. Mu, R.P. Hermann, S. Gorsse et al., Phys. Rev. Mater. **3**, 025403 (2019)
4. M.E. Schlesinger, J. Phase Equilibria **9**, 591 (1998)
5. L.M. Sandratskii, R.F. Egorov, A.A. Berdyshev, Phys. Status Solidi (b) **104**, 103–107 (1981)
6. A.I. Zviagin, L.V. Povstoanyi, P.M. Arefieva, Izv. Akad. Nauk SSSR **35**, 1190 (1971)
7. J. Dong, F.-H. Sun, H. Tang et al., ACS Appl. Mater. Interfaces **11**, 28221 (2019)
8. R.R. Heikes, R.W. Ure, *Thermoelectricity: science and engineering* (Interscience Publishers, Geneva, 1961)
9. Y. Xu, W. Li, C. Wang et al., J. Mater. Chem. A **5**, 19143 (2017)
10. G.R. Wu, K. Nagatomo, M. Sasaki et al., Solid State Comm. **118**, 425 (2001)
11. S. Ahmad, K. Hoang, S.D. Mahanti, Phys. Rev. Lett. **96**, 056403 (2006)
12. G. Tang, W. Wei, J. Zhang et al., J. Am. Chem. Soc. **138**, 13647 (2016)
13. K.F. Hsu, S. Loo, F. Guo et al., Science **303**, 818 (2004)
14. J.R. Sootsman, D.Y. Chung, M.G. Kanatzidis, Ang. Chem. Int. Ed. **48**, 8616 (2009)
15. B. Kim, I. Kim, B. Min et al., Electron. Mater. Lett. **9**, 477 (2013)
16. L.-B. Zhang, H.-L. Qi, J.-L. Gao et al., J. Electron. Mater. **46**, 2894 (2017)
17. A. Basit, J. Yang, Q. Jiang et al., J. Alloys Comp. **777**, 968 (2019)
18. A. Basit, J. Yang, Q. Jiang et al., J. Mater. Chem. A **6**, 23473 (2018)
19. J. Dong, C.-F. Wu, J. Pei et al., J. Mater. Chem. C **6**, 4265 (2018)
20. J. Dong, J. Pei, K. Hayashi et al., J. Materiomics **7**, 577 (2021)
21. G. Tan, F. Shi, S. Hao et al., J. Am. Chem. Soc. **137**, 11507 (2015)
22. Z. Zheng, X. Su, R. Deng et al., J. Am. Chem. Soc. **140**, 2673 (2018)
23. S. Welzmiller, F. Heinke, P. Huth et al., J. Alloys Comp. **652**, 74 (2015)

24. A. Slebarski, M.B. Maple, E.J. Freeman et al., Phys. Rev. B **62**, 3296 (2000)
25. A.I. Voronin, VYu. Zueva, DYu. Karpenkov et al., Semiconductors **51**, 891 (2017)
26. A.I. Taranova, A.P. Novitskii, A.I. Voronin et al., Semiconductors **53**, 768 (2019)
27. H. Nakatsugawa, T. Ozaki, H. Kishimura, Y. Okamoto, J. Electron. Mater. **49**, 2802 (2020)
28. A. Novitskii, I. Serhiienko, A. Nepapushev et al., Intermetallics **133**, 107195 (2021)